Stable moving patterns in the 2-D Gray-Scott model

Robert Munafo

Version 0.33, 2009 April 10.

Abstract

We show stable single and multi-spot patterns of three classes: stationary, rotating, and moving, that exist within a limited range of parameter values in the 2-dimensional Gray-Scott reaction-diffusion model. These patterns appear to derive their stability from a constructive reinforcement effect of the standing waves that surround any feature. Several other examples of combined stability and motion are noted, with suggestions for further research.

Introduction

The Gray-Scott model [2] is a widely-studied model of a pair of reactions in a stirred tank. It has been applied in reaction-diffusion models in one [7, 10, 11, 14], two [4, 10, 12, 13, 17, 18] and three [15] dimensions. Widely-known results include the existence of stable spot patterns, self-replication of spots, spontaneous formation of stripes and hexagonal arrays, and a great similarity to Turing patterns. Findings that show a lack of moving stable patterns, e.g. [7] apply only in 1-D or a limited region of the 2-D system parameter space ([10] p. 81).

The model equations are:

$$\frac{\partial U}{\partial t} = D_u \nabla^2 U - UV^2 + F(1 - U),$$
$$\frac{\partial V}{\partial t} = D_v \nabla^2 V + UV^2 - (F + k)V \tag{1}$$

This paper discusses the two-dimensional case, using the terminology and symbols of Pearson [4]. The parameters F and k represent the feed rate and removal rate of the reactants U and V. We refer to the dimensionless units of length and time in (1) by lu and tu respectively.

1 Methods

We used numerical simulation similar to that used by [4]. All figures shown here were produced with a 256×256 grid, representing a system size of $1.79\text{lu} \times 1.79\text{lu}$, with parameters $D_u = 2 \times 10^{-5}$, $D_v = 10^{-5}$, periodic boundary conditions, and a time step of 0.5 tu per calculation step.

To verify the results, we used grids as large as 2048×2048 representing system sizes up to 10×10, time steps down to 0.03 tu and IEEE double precision; there was no qualitative difference in the results. The same results also appear at Pearson's grid resolutions of 102 grid points per lu and 1 computation step per tu.

The initial state was created in several ways. Most results were produced by starting with a background level of U and V set to a homogeneous state computed from F and k. Transforming the variables and units from Muratov and Osipov[10], the third homogeneous state θ_{h3} exists when $k < (\sqrt{F} - 2F)/2$, with U and V given by

$$ U = \frac{A - \sqrt{A^2 - 4}}{2A} \qquad\qquad V = \frac{\sqrt{F}(A + \sqrt{A^2 - 4})}{2} \tag{2} $$

where the dimensionless A is $\sqrt{F}/(F + k)$. Starting with a grid filled with these values of U and V or with the trivial state $U = 0$, $V = 1$, a number of rectangles were added whose width, height, locations, and number were determined randomly, and then filled with random levels of U and V. A repeatable pseudo-random algorithm was used and the initial seed values saved so the same simulation sequence could be reproduced at will [8]. The system was then solved numerically for anywhere from 10^5 to 5×10^8 tu, as needed for the phenomena under test.

Although all of the patterns shown here arose naturally from such initial random states, a number of techniques were used to make exploration and discovery more practical: Selectively clearing unwanted patterns by setting portions of the grid to the homogeneous state; combining parts of patterns to create others; changing F and k parameters; moving small parts of the grid to test pattern integrity; then continuing the simulation after making any of these changes.

Because of their stability, each of the patterns reported here will naturally evolve from any starting pattern that superficially resembles it, provided the dimensions and levels of U and V are approximately correct.

We found it exceptionally useful to visualize U and $\partial U/\partial t$ simultaneously via appropriate color mappings, with the latter greatly amplified to distinguish its sign even when its magnitude is nearly zero. Additional insight was also gained from 1-D and 3-D numerical simulations.

2   Principal Findings

We noted all of the pattern types reported in [4], and three more which are named in figure 1, extending the classification letters of Pearson.

Type ν is found throughout the large area labeled **R** by Pearson. Here we have static stable spots (called autosolitons by others [10]) that do not multiply. At lower F values the spots oscillate with a characteristic frequency and damping rate that is constant for any given F and k. As one increases F towards the frontier of viability for these spots the stable state becomes smaller in diameter and the central peak has a higher value of V.

| | (a) $F = 0.040$, $k = 0.070$ | (b) $F = 0.014$, $k = 0.047$ | (c) $F = 0.060$, $k = 0.0609$ |

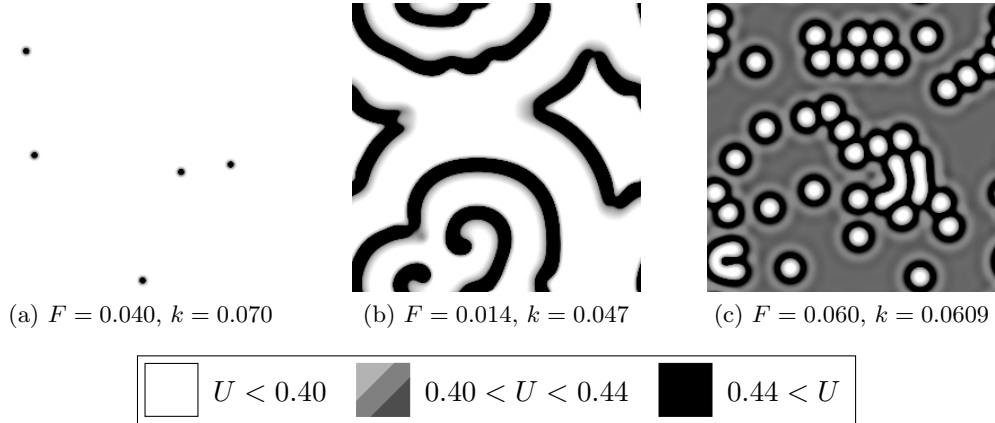| $U < 0.40$ | $0.40 < U < 0.44$ | $0.44 < U$ |

Figure 1: Pattern types ν (static non-replicating autosolitons), ξ (B-Z targets and spirals), and π (stable, stationary and moving inverted patterns).

Type ξ is found in a fairly large area around $F = 0.014$ and $k = 0.047$. These patterns very closely resemble the B-Z (Belousov-Zhabotinsky) reaction in a Petri dish. A proto-spiral seed of some type in the initial pattern will produce sustained spiraling patterns.

Type π is the most novel and the subject of the rest of our discussion. We found these patterns for F values ranging from 0.04 to 0.09, in a thin band of k values. The band runs roughly parallel to the saddle-node and Hopf bifurcation lines, and at lower k values. It is also at lower k values than the area investigated by McGough and Riley [17]. At all F values the band is very narrow in k as compared to its distance from the bifurcation lines. For example, when $F = 0.06$, the Hopf bifurcation is at $k \approx 0.06247$, and the range of valid k values for the object in the lower-left of figure 2a was found numerically to be $0.06084 \pm 0.00001 \leq k \leq 0.06092 \pm 0.00001$.

3   Stability of type π Patterns

Figure 2a shows five patterns, visualized by their values of U and $\partial U / \partial T$. The three in the upper row are stable non-moving patterns. Contrast has been exaggerated in the area of $0.40 < U < 0.44$ to show the concentric ring patterns that surround all patterns of this type.

The other two patterns in figure 2a move to the left, indefinitely at constant speed; the three-spot pattern moves at about 1 lu per 8×10^6 tu, and the U-shaped pattern at about 1 lu per 1.25×10^5 tu.

All of the patterns in 2a arise frequently from random starting patterns, and are resilient to noise and other perturbations. If any of them is perturbed by shifting half of the pattern in any direction a distance on the order of 0.02 lu, further simulation results in a return to the canonical forms shown here.

Figure 2b shows the time derivative of U. The motion of the two patterns in the bottom half of

3

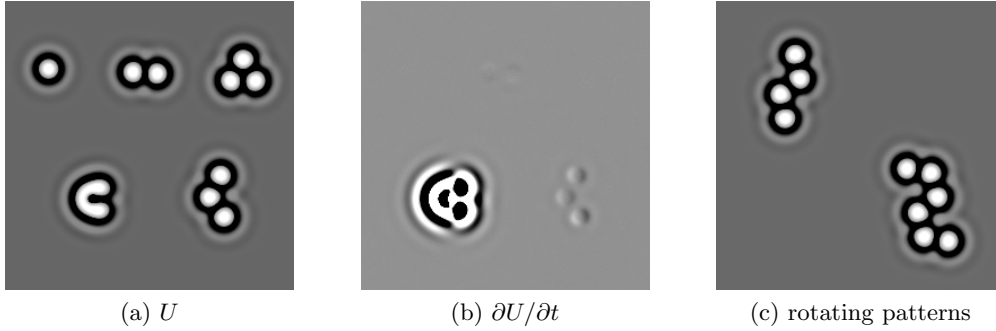|		
(a) U	(b) $\partial U/\partial t$	(c) rotating patterns

Figure 2: Comparison of U to its time derivative for pattern type π. Coloring for the left figure is the same as above. In the center image, white represents $\partial U/\partial t > 10^{-5}$; gray where $|\partial U/\partial t| < 10^{-5}$, and black otherwise.

the figure is clear. Figure 2c shows two rotating patterns. Both rotate clockwise; the one in the upper-left performs one full revolution in about 1.6×10^7 tu; the other takes about 1.2×10^7 tu.

4 Diversity of Behavior

The patterns in figure 2a are shown as they appear when $F = 0.06$ and $k = 0.0609$. If k is diminished below 0.060884, the U-shaped moving pattern is no longer viable. When $k < 0.06062$ the single spot shown in the upper-left of figure 2a is no longer stable and quickly evolves to the homogeneous state, however the other three patterns made up of spots continue to exist. When k is lowered below 0.06060, the patterns in the top center and lower right vanish, but the triangular three-spot pattern remains. Below 0.06057 the triangular pattern vanishes, but a 7-spot arrangement similar to that in figure 4c is still viable. The 7-spot pattern dies out when $k < 0.06055$.

Figures 3a and 3b show two points in a simulation in which k was gradually increased from 0.06058 to 0.06110 over 10^6 tu. The overall length of the horizontal row of spots increases with k, and the smaller 3-spot pattern moves slightly away from it. The entire set of 15 spots also rotates very slowly as a unit. Similar interactions between patterns that are not in direct contact are very common. Decreasing k back to 0.06058 over a similar time period causes the pattern to return to the state in 3a.

Figure 3c shows some features that exhibit stable parallel stripe spacing. In the upper pattern, the larger circular portion is a pattern that arises frequently from circular and ring-shaped starting patterns. It can occur alone or with one or more extra spots as seen here. Many such patterns have long-term stability and the one shown here moves to the right at about 1 lu per 3.5×10^6 tu. The bottom shows another of these ring features after having been distorted by the stripe above it. The stripe is a very common feature, and grows quickly from both ends. While growing it tends to remain parallel to other features; the curved path seen here results from it following the edges of the ring and spots. It also causes features like the ring to lose their stability; from the state shown here the ring grows slowly towards the left. If allowed to proceed, patterns with active growing
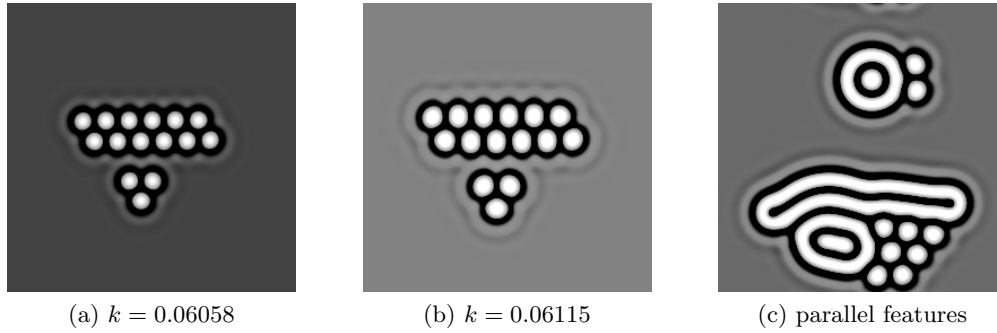
4

(a) $k = 0.06058$ (b) $k = 0.06115$ (c) parallel features

Figure 3: Lattice spacings and parallel features.. $F = 0.06$ for all figures. Coloring is the same as above.

(a) $k = 0.0609$ (b) $k = 0.0611$ (c) $k = 0.06135$ (d) $k = 0.0615$
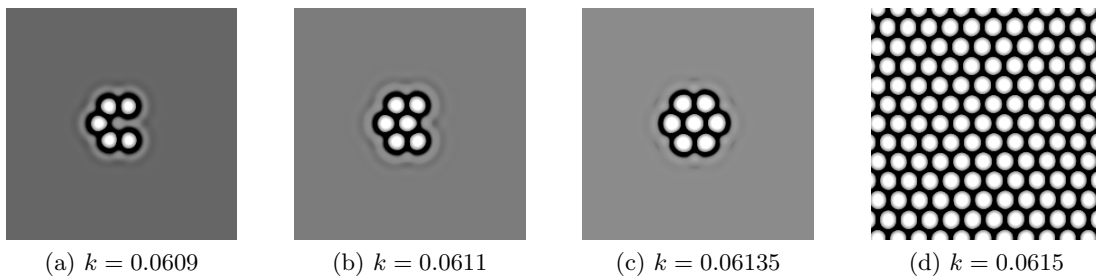
Figure 4: Evolution of a starting pattern at three nearby parameter values. $F = 0.06$ for all figures. Coloring is the same as above.

stripes will usually grow to fill all available space with spots and stripes, but the time taken and the final proportion of spots to stripes is highly variable, depending on tiny details of the initial configuration.

At $F = 0.06, k = 0.0609$ the 5-spot pattern in figure 4a is stable and moves to the left slowly. Using this as the starting pattern, k is increased to 0.0611, and a spot forms in the center to make the 6-spot pattern in figure 4b. This pattern is also left-moving and stable. Increasing k further to 0.06135, a seventh spot appears (figure 4c), and motion stops due to the attainment of symmetry. Throughout this process the spots shift away from one another slightly to attain a new steady state, with a slightly greater inter-spot spacing with each increase in k. When k is increased to 0.0615, new spots appear on all sides, quickly growing to produce the uniform hexagonal grid in figure 4d. Combined with the limited viability of smaller groups of spots described above, there is a wide spectrum of patterns and phenomena in the relatively narrow band $0.06055 < k < 0.0615$. A similar spectrum is found at higher and lower F values.

5

5 Discussion

The single spot in upper-left of figure 2a has a set of concentric halos with progressively lower amplitude and alternating sign. In multi-spot patterns, each spot tends to be found at a location that coincides with the first positive-sign surrounding halo. In the growth of hexagonal arrays, the new spots always appear at such locations.

In figure 2a, note that the U-shaped moving pattern is of similar size and shape to the three-spot pattern, and that both tend to return to the canonical dimensions shown here after an induced distortion.

In more distant alignments such as that in figure 3a the spots are found at distances coinciding with each other's second positive-signed surrounding halos. This is also evident in the five-spot pattern in figure 4a, which remains as shown when perturbed, rather than changing to a pentagonal ring or some other arrangement.

In figure 3, the concentric halos appear in some places as roughly linear features; the path of the growing stripe closely follows the location of these linear halos.

All of the foregoing phenomena seem to suggest that all areas of high U produce a pattern of surrounding standing waves, and that these standing waves combine in a nearly linear way to produce an effect of constructive and destructive interference. Analytical research is needed to establish a basis for this theory, or another explanation that can account for the observed phenomena. Similar effects were observed in 1-D numerical simulation; analytical work can probably begin there.

There is much opportunity for further research by numerical simulation, including rigorous statistical analysis to establish the degree of stability of the patterns in response to varying levels of perturbation stimuli. We observed a large variety of patterns and interactions similar to those reported here, and there is a likelihood that changing the other parameters in the Gray-Scott equations (specifically F and D_u/D_v) will also yield new discoveries.

Acknowledgments

References

[1] A. M. Turing, The chemical basis of morphogenesis, *Philosophical Transactions of the Royal Society of London, Series B (Biological Sciences)*, **237(641)**, 37-72 (1952).

[2] P. Gray and S.K. Scott, Autocatalytic reactions in the isothermal, continuous stirred tank reactor: isolas and other forms of multistability, *Chem. Eng. Sci.* **38** 29-43 (1983)

[3] Q. Ouyang and H. L. Swinney, Transition from a uniform state to hexagonal and striped Turing patterns, *Nature* **352**, 610-612 (1991).

[4] J. Pearson, Complex patterns in a simple system, *Science* **261**, 189-192 (1993).

[5] K. J. Lee, W. D. McCormick, Q. Ouyang, and H. L. Swinney, Pattern formation by interacting chemical fronts, *Science* **261**, 192-194 (1993).

[6] K. J. Lee, W. D. McCormick, H. L. Swinney, and J. E. Pearson, Experimental observation of self-replicating spots in a reaction-diffusion system, *Nature* **369**, 215-218 (1994).

[7] A. Doelman, T. J. Kaper, and P. A. Zegeling, Pattern formation in the 1-D Gray-Scott model, *Nonlinearity* **10**, 523-563 (1997).

[8] D. E. Knuth, *The Art of Computer Programming*, **2** (Seminumerical Algorithms), 184-189 (1997).

[9] A. Doelman, R. A. Gardner, and T. J. Kaper, Stability analysis of singular patterns in the 1-D Gray-Scott I: A matched asymptotics approach, *Physica D* **122**, 1-36 (1998).

[10] C. B. Muratov and V. V. Osipov, Spike autosolitons in the Gray-Scott model, CAMS Rep. 9900-10, NJIT, Newark, NJ (available at arXiv.org: patt-sol/9804001).

[11] Y. Nishiura and D. Ueyama, Self-Replication, Self-Destruction, and Spatio-Temporal Chaos in the Gray-Scott Model, *Physical Review Letters* **15**, 281-289 (2000).

[12] M. Stich, Target patterns and pacemakers in reaction-diffusion systems, Doctoral thesis, Technical University of Berlin, 2003.

[13] J. Wei and M. Winter, Existence and stability of multiple-spot solutions for the Gray-Scott model in R^2, *Physica D: Nonlinear Phenomena* **176 (3-4)**, 147-180 (2003).

[14] T. Kolokolnikov, Pattern formation in reaction-diffusion models far from the Turing regime, Doctoral thesis, University of British Columbia, August 2004.

[15] T. Leppänen, Computational Studies of Pattern Formation in Turing Systems, Doctoral thesis, Helsinki University of Technology, November 2004.

[16] H. Mahara, N. Suematsu, T. Yamaguchi, K. Ohgane, Y. Nishiura, and M. Shimomura, Three-variable reversible Gray-Scott model *The Journal of Chemical Physics* **121(18)**, 8968-8972 (2004)

[17] J. S. McGough and K. Riley, Pattern formation in the Gray-Scott model, *Nonlinear Analysis: Real World Applications* **5(1)**, 105-121 (2004)

[18] A. Munteanu and R. V. Sole, Pattern Formation in Noisy Self-Replicating Spots *International Journal of Bifurcation and Chaos* **12(16)**, 3679-3685 (2006)